Mon. Not. R. Astron. Soc. **000**, 000–000 (0000) Printed 15 September 2014 (MN LATEX style file v2.2)

Parity-odd correlators of diffuse gamma rays and intergalactic magnetic fields

Hiroyuki Tashiro* and Tanmay Vachaspati†
*Department of Physics and Astrophysics, Nagoya University, Nagoya 464-8602, Japan.
†Physics Department, Arizona State University, Tempe, Arizona 85287, USA.

arXiv:1409.3627v1 [astro-ph.CO] 12 Sep 2014

15 September 2014

ABSTRACT

We develop the connection between intergalactic helical magnetic fields and parity odd signatures in the diffuse gamma ray sky. We find that the location and the amplitude of a peak in a parity odd correlator, $Q(R)$, can be used to infer the normal and helical power spectra of the intergalactic magnetic field. When applied to Fermi-LAT data, the amplitude of the observed peak in $Q(R)$ gives $\sim 10^{-14}$ G intergalactic magnetic field strength, which is consistent with an earlier independent estimate that only used the peak location (Tashiro et al. 2014). We discuss features in the observed $Q(R)$ that further support the intergalactic magnetic field hypothesis and make predictions for future tests.

1 INTRODUCTION

It has been known for some time that gamma rays from TeV blazars can probe the intergalactic magnetic field (Aharonian et al. 1994; Plaga 1995; Neronov & Semikoz 2007; Elyiv et al. 2009; Dolag et al. 2009; Neronov & Semikoz 2009). Photons with TeV energy from such beamed sources scatter off the extra-galactic background light (EBL) and produce electron-positron pairs also with TeV energy (Gould & Schréder 1966; Aharonian et al. 2006). These charged particles then inverse-Compton scatter off cosmic microwave background (CMB) photons and up-scatter them to a cascade of GeV photons. These GeV gamma rays potentially carry information about the electron-positron trajectories. In particular, if the electron-positron are deflected by ambient magnetic fields, the cascade gamma rays observed at GeV energies also carry information about the ambient magnetic fields.

A few years ago, observations of four TeV blazars by the Fermi Large Area Telescope (Fermi-LAT) experiment[1] and the High Energy Stereoscopic System (HESS) gamma ray telescope[2] were used to obtain a lower bound of $\sim 10^{-16}$ G on the intergalactic magnetic field strength (Neronov & Vovk 2010; Tavecchio et al. 2010; Dolag et al. 2011). The conclusion is based on the observed deficit of GeV photons, the assumption being that the deficit is due to deflection of the electron-positron pairs due to an inter-galactic magnetic field. The assumption has since been debated (Broderick et al. 2012; Miniati & Elyiv 2013; Schlickeiser et al. 2012), with the concern that there is an instability in the propagation of high energy charged particles in the cosmological medium that tends to isotropize the directions of the charged particles thus explaining the observed deficit of GeV photons.

More recently, developing ideas first proposed in the context of cosmic rays (Kahniashvili & Vachaspati 2006), we have shown that the cascade GeV gamma rays from TeV blazars may also be used to probe *helical* magnetic fields as the helicity introduces a parity odd signature in the arrival directions of the gamma rays (Tashiro & Vachaspati 2013). If observed, a parity violating signal around blazars would be hard to explain on the basis of a plasma instability but easier to explain with magnetic field helicity. In turn, primordial magnetic field helicity would be an invaluable probe of CP violation in the early universe with profound consequences for very high energy particle physics and the origin of matter (Vachaspati 2001; Copi et al. 2008; Chu et al. 2011; Long et al. 2014). A magnetic field in the post-recombination universe can be a critical ingredient that enables cosmic structure formation (Rees 1987).

Most recently, we have extended the scheme to look for parity odd signatures in gamma rays from a single source to the

[1] http://fermi.gsfc.nasa.gov
[2] http://www.mpi-hd.mpg.de/hfm/HESS/

© 0000 RAS

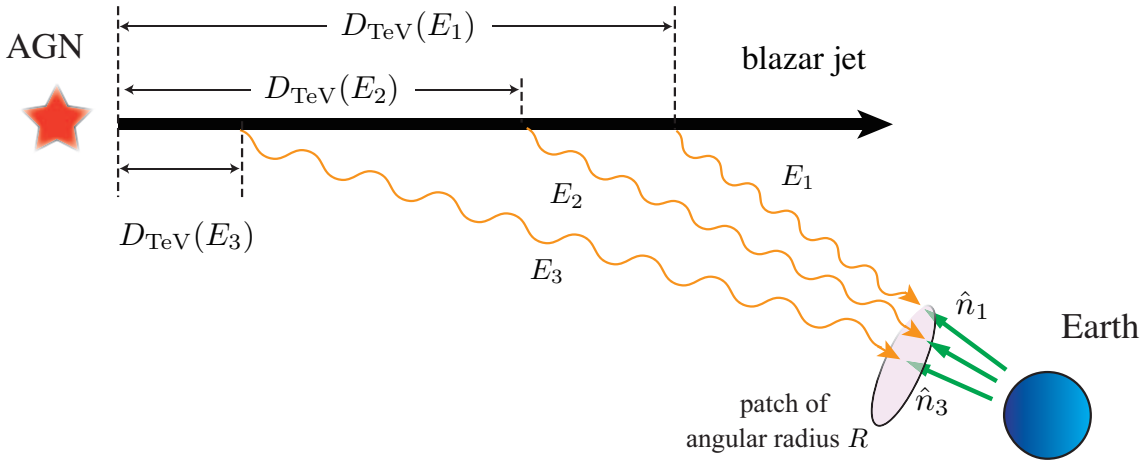

Figure 1. A collimated jet emanates from the source AGN. Very high energy photons propagate a short distance, $D_{\rm TeV}(E_3)$, and then pair-produce. The charged pairs propagate a very short distance (too small to be shown) and then inverse Compton scatter CMB photons to GeV energies that are then observed to come from a direction $\hat{\boldsymbol{n}}_3$. Lower energy photons from the source propagate a larger distance, $D_{\rm TeV}(E_1)$, before producing pairs, that then produce cascade photons seen to come from direction $\hat{\boldsymbol{n}}_1$. The statistics, $Q(R)$, is the average of the triple product of the vectors $\hat{\boldsymbol{n}}_1$, $\hat{\boldsymbol{n}}_2$ (not labeled in the diagram) and $\hat{\boldsymbol{n}}_3$ in a patch of radius R where $E_3 > E_2 > E_1$.

diffuse gamma ray background over the entire sky (Tashiro et al. 2014). This extension is particularly necessary if the cascade deflections are large and the observed GeV gamma rays are not obviously associated with any TeV blazar source. Further, we have applied our scheme to the diffuse gamma rays observed by Fermi-LAT, and find a significant parity odd signal. Interpreted in terms of a helical magnetic field, we find a field strength $\sim 10^{-14}$ G on intergalactic scales with left-handed helicity.

If ongoing observations continue to confirm the parity odd signal, we should be able to use the gamma ray signal to reconstruct spectral properties of the intergalactic field. More specifically, the equal-time correlation function of a stochastic, isotropic, magnetic field in Minkowski spacetime can be written as (Monin & I'Aglom 1971)

$$\langle B_i(\boldsymbol{x})B_j(\boldsymbol{y})\rangle = M_N(r)\left(\delta_{ij} - \frac{r_i r_j}{r^2}\right) + M_L(r)\frac{r_i r_j}{r^2} + M_H(r)\epsilon_{ijl}r^l, \tag{1}$$

where $\boldsymbol{r} = \boldsymbol{x} - \boldsymbol{y}$ and, due to the divergence free condition of magnetic fields,

$$M_N(r) = \frac{1}{2r}\frac{d}{dr}(r^2 M_L(r)). \tag{2}$$

We would like to relate the "normal" and "helical" power spectra, M_N and M_H, to correlators of the observed cascade GeV gamma rays. In Tashiro et al. (2014), we had related $M_H(r)$ to a parity odd correlator of cascade gamma rays from a known source. In the present paper we will extend that analysis to the case of diffuse gamma rays, when the source locations are not known. Further, if $M_H \neq 0$, it allows for a new way to also estimate the normal power spectrum from correlation functions of cascade gamma rays.

In Sec. 2 we will introduce our strategy in more detail, first in the context of a single source, then in the context of many sources and when additional non-cascade photons are present in the data. We will find that the parity odd signal can be a valuable tool for extracting information not just about the magnetic field but also about the relative number of cascade and non-cascade photons, which is related to the number of TeV blazars. In Sec. 3 we make predictions for the parity odd signal if the magnetic field correlator has a simple power law form. We conclude in Sec. 4 where we also discuss limitations of the present analysis. In Appendix A we relate the sign of the parity odd statistic to the handedness of the magnetic field.

2 PARITY ODD CORRELATORS OF GAMMA RAYS

Consider a TeV blazar at redshift z_s. The emitted TeV gamma rays interact with the EBL to produce electron-positron pairs over a mean free path (Neronov & Semikoz 2009) (see Fig. 1)

$$D_{\rm TeV}(E_{\rm TeV}) \sim 80\frac{\kappa}{(1+z_s)^2}\ {\rm Mpc}\ \left(\frac{E_{\rm TeV}}{10\ {\rm TeV}}\right)^{-1}, \tag{3}$$

where κ is a numerical factor which accounts for the model uncertainties of EBL. Here we take $\kappa \sim 1$ (Neronov & Semikoz 2009).

Electron-positron pairs generated by the TeV gamma ray lose energy by IC scattering off CMB photons over a dis-

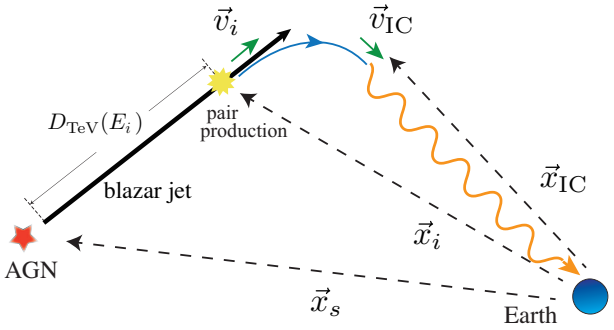

Figure 2. The TeV gamma ray from a blazar pair produces at $\boldsymbol{x}_i$ and the pair has velocity $\boldsymbol{v}_i$. The pair bend in the magnetic field (only the e^+ trajectory is shown) and then inverse Compton at $\boldsymbol{x}_{IC}$ when the velocity is $\boldsymbol{v}_{IC}$. The constraint is that the up-scattered CMB photon, now at GeV energy and propagating along $\boldsymbol{v}_{IC}$ reaches Earth. This gives the constraint equation: $\boldsymbol{v}_{IC} = -\hat{\boldsymbol{x}}_{IC}$, where we choose the origin of the coordinate system to be located at Earth.

tance (Neronov & Semikoz 2009)

$$D_e \sim 30 \text{ kpc } (1+z_e)^{-4} \left(\frac{E_e}{10 \text{ TeV}}\right)^{-1}, \tag{4}$$

where z_e is the typical redshift at which TeV gamma rays create pairs, and $E_e \sim E_{\rm TeV}/2$ is the electron energy. The secondary gamma ray cascade contains up-scattered CMB photons with typical energy

$$E_\gamma = \frac{4}{3}(1+z_e)^{-1}\epsilon_{CMB}\left(\frac{E_e}{m_e}\right)^2 \sim 88 \text{ GeV } \left(\frac{E_{\rm TeV}}{10 \text{ TeV}}\right)^2, \tag{5}$$

where $\epsilon_{\rm CMB} = 6\times 10^{-4}(1+z_e)$ eV is the typical energy of CMB photons.

The angle by which gamma rays are bent with respect to the source direction is given by (Tashiro & Vachaspati 2013)

$$\Theta(E_\gamma) \approx \frac{qD_{\rm TeV}D_e}{E_e D_s}\, v_L B \approx 7.3\times 10^{-5} \left(\frac{B_0}{10^{-16}\text{ G}}\right)\left(\frac{E_\gamma}{100 \text{ GeV}}\right)^{-3/2}\left(\frac{D_s}{1000 \text{ Mpc}}\right)^{-1}(1+z_s)^{-4}, \tag{6}$$

where q is the electron charge and $v_L \sim 1$ is the speed. To obtain the redshift dependence we take the redshifts of the pair production event, z_e, to be approximately the redshift to the source, z_s, and $B_0 = B/(1+z_e)^2$ as expected from flux conservation.

In the following subsection, we will consider cascade photons of three different energies $E_1 < E_2 < E_3$ with arrival directions $\boldsymbol{n}(E_1)$, $\boldsymbol{n}(E_2)$ and $\boldsymbol{n}(E_3)$ (see Fig. 1) and evaluate the correlator

$$Q_\infty = \langle \boldsymbol{n}(E_1)\times\boldsymbol{n}(E_2)\cdot\boldsymbol{n}(E_3)\rangle, \tag{7}$$

for a single source. This is a special case of the correlator for diffuse background of gamma rays that was considered in (Tashiro et al. 2014)

$$Q(R) = \langle \boldsymbol{n}(E_1)\times\boldsymbol{n}(E_2)\cdot\boldsymbol{n}(E_3)\rangle_R, \tag{8}$$

in which only photons within an angular distance R from $\boldsymbol{n}(E_3)$ were included in the ensemble average and then an average over all locations of $\boldsymbol{n}(E_3)$ was taken. In other words, the ensemble average was taken over photons such that $\boldsymbol{n}(E_1)\cdot\boldsymbol{n}(E_3) > \cos R$ and $\boldsymbol{n}(E_2)\cdot\boldsymbol{n}(E_3) > \cos R$ for all locations, $\boldsymbol{n}(E_3)$, on the sky.

2.1 A single unidentified source

We imagine a single beamed source of TeV gamma rays that is positioned in a general way – the Earth may or may not lie within the opening angle of the jet. Even if Earth is located outside the jet, cascade photons from the source can still get to Earth if intergalactic magnetic fields are present because the trajectories of the electron-positron pairs will bend in the magnetic field as illustrated in Fig. 2. We will consider this situation.

Let us denote the location of the source by $\boldsymbol{x}_s$. A $\sim$ TeV energy photon propagates a distance $D_{\rm TeV}$ with velocity $\boldsymbol{v}_i$ and then pair produces an electron-positron pair at $\boldsymbol{x}_i$, at time t_i, given by

$$\boldsymbol{x}_i = \boldsymbol{x}_s + D_{\rm TeV}\boldsymbol{v}_i. \tag{9}$$

The electron-positron then propagate in a weak magnetic field which causes their trajectories to bend. However, the bending is weak, and for the up-scattered CMB photons to arrive at Earth, the velocity of the positron (say) at time t_i has to approximately point to the Earth. Hence at time t_i we can write,

$$\boldsymbol{v}_i = -\hat{\boldsymbol{x}}_i + \delta\boldsymbol{v}_i, \tag{10}$$

with $\hat{\boldsymbol{x}}_i \cdot \delta\boldsymbol{v}_i = 0$.

After propagating up to the time of inverse Compton scattering, at time t_{IC}, the velocity and position of one of the pair – assumed positron – is (the other member of the pair gets lost),

$$\boldsymbol{v}_{IC} = \boldsymbol{v}_i + q\frac{\boldsymbol{v}_i}{E} \times \boldsymbol{b}, \tag{11}$$

$$\boldsymbol{x}_{IC} = \boldsymbol{x}_i + \boldsymbol{v}_i T + q\frac{\boldsymbol{v}_i}{E} \times \boldsymbol{c}, \tag{12}$$

where E is the energy of the electron/positron, $q = +e$ is the positron's electric charge, $T = t_{IC} - t_i$,

$$\boldsymbol{b} = \int_{t_i}^{t_{IC}} dt' \ \boldsymbol{B}(\boldsymbol{x}_i + \boldsymbol{v}_i(t' - t_i)), \tag{13}$$

$$\boldsymbol{c} = \int_{t_i}^{t_{IC}} dt' \int_{t_i}^{t'} dt'' \ \boldsymbol{B}(\boldsymbol{x}_i + \boldsymbol{v}_i(t'' - t_i)). \tag{14}$$

Note that we are using the unperturbed trajectory when doing the integration. This is legitimate since we are working to lowest order in $|\boldsymbol{B}|$.

The constraint is that the GeV photon should arrive to Earth. So

$$\boldsymbol{v}_{IC} = -\hat{\boldsymbol{x}}_{IC}. \tag{15}$$

This gives

$$\boldsymbol{v}_i + q\frac{\boldsymbol{v}_i}{E} \times \boldsymbol{b} = -\frac{1}{r_{IC}}\left(\boldsymbol{x}_i + \boldsymbol{v}_i T + q\frac{\boldsymbol{v}_i}{E} \times \boldsymbol{c}\right). \tag{16}$$

Ignoring terms of quadratic and higher order in $\delta\boldsymbol{v}_i$, $\boldsymbol{B}$, and also assuming $T \ll r_{IC} \sim |\boldsymbol{x}_i| = r_i$ – typically $T \sim 30$ kpc, $r_i \sim 1$ Gpc – gives

$$\delta\boldsymbol{v}_i \approx q\frac{\hat{\boldsymbol{x}}_i}{E} \times \left(\boldsymbol{b} + \frac{\boldsymbol{c}}{r_i}\right). \tag{17}$$

This is the constraint on the initial velocity so that the GeV gamma ray reaches Earth. Straight-forward algebra now gives us the arrival direction of the photon

$$\begin{aligned}
\boldsymbol{n}(E) \equiv -\boldsymbol{v}_{IC}(E) =& -\boldsymbol{v}_i - q\frac{\boldsymbol{v}_i}{E} \times \boldsymbol{b} \\
=& \hat{\boldsymbol{x}}_i - \delta\boldsymbol{v}_i - q\frac{\boldsymbol{v}_i}{E} \times \boldsymbol{b} \\
\approx& \hat{\boldsymbol{x}}_i - q\frac{\hat{\boldsymbol{x}}_i}{E} \times \left(\boldsymbol{b} + \frac{\boldsymbol{c}}{r_i}\right) + q\frac{\hat{\boldsymbol{x}}_i}{E} \times \boldsymbol{b} \\
=& \hat{\boldsymbol{x}}_i - q\frac{\hat{\boldsymbol{x}}_i}{E} \times \frac{\boldsymbol{c}}{r_i}.
\end{aligned} \tag{18}$$

Next we insert the expression for $\boldsymbol{n}$ in the definition of Q_∞ in Eq. (7) and ignore linear and cubic terms in $\boldsymbol{B}$ to get

$$Q_\infty = \langle \hat{\boldsymbol{x}}_{i1} \times \hat{\boldsymbol{x}}_{i2} \cdot \hat{\boldsymbol{x}}_{i3} \rangle + \sum_{\text{cyc.}} \frac{q_1 q_2}{E_e(E_1) E_e(E_2) r_{i1} r_{i2}} \langle (\hat{\boldsymbol{x}}_{i1} \times \boldsymbol{c}_1) \times (\hat{\boldsymbol{x}}_{i2} \times \boldsymbol{c}_2) \cdot \hat{\boldsymbol{x}}_{i3} \rangle, \tag{19}$$

where the $1, 2, 3$ subscripts refer to particles of energies E_1, E_2, E_3 and charges q_1, q_2, q_3; the sum is over cyclic perturbations of $1, 2, 3$, and the subscript i refers to the initial moment, at the time the TeV photon produces pairs. Eq. (19) is the expression for Q_∞ to quadratic order in the magnetic field.

Note that the first term in Eq. (19) also depends on the magnetic field through the constraint conditions Eq. (9) and Eq. (15). In fact we shall show in a moment that the second term is much smaller than the first. Focussing on the first term, using Eq. (9), we can write

$$\langle \hat{\boldsymbol{x}}_{i1} \times \hat{\boldsymbol{x}}_{i2} \cdot \hat{\boldsymbol{x}}_{i3} \rangle \approx \frac{1}{D_s^3} \langle (\boldsymbol{x}_s + D_{\text{TeV}1}\boldsymbol{v}_{i1}) \times (\boldsymbol{x}_s + D_{\text{TeV}2}\boldsymbol{v}_{i2}) \cdot (\boldsymbol{x}_s + D_{\text{TeV}3}\boldsymbol{v}_{i3}) \rangle, \tag{20}$$

where we have approximated $|\boldsymbol{x}_i| \approx D_s$. The initial velocities depend on $\delta\boldsymbol{v}_i$ in Eq. (10), which in turn depend on the magnetic field via Eq. (17). Then, noting that $D_{\text{TeV}}/D_s \ll 1$, we find

$$\langle \hat{\boldsymbol{x}}_{i1} \times \hat{\boldsymbol{x}}_{i2} \cdot \hat{\boldsymbol{x}}_{i3} \rangle \approx \sum_{(a,b)} \frac{D_{\text{TeV,a}} D_{\text{TeV,b}}}{D_s^2} \langle \delta\boldsymbol{v}_{ia} \times \delta\boldsymbol{v}_{ib} \rangle \cdot \hat{\boldsymbol{x}}_s, \tag{21}$$

where the sum is over $(a, b) = (1, 2), (2, 3), (3, 1)$. Now we can insert expressions for $\delta\boldsymbol{v}_{ia}$ using Eq. (17). The algebra simplifies because

$$|\boldsymbol{b}| = O(D_e B) \gg \frac{|\boldsymbol{c}|}{r_i} = O\left(\frac{D_e^2 B}{D_s}\right), \tag{22}$$

where we recall $D_e \sim 30$ kpc and $D_s \sim$ Gpc. Then, to lowest order in D_e/D_s and D_{TeV}/D_s we obtain

$$\langle \hat{\boldsymbol{x}}_{i1} \times \hat{\boldsymbol{x}}_{i2} \cdot \hat{\boldsymbol{x}}_{i3} \rangle \approx \sum \frac{q_a q_b D_{\text{TeV,a}} D_{\text{TeV,b}}}{E_e(E_a) E_e(E_b) D_s^2} \langle \boldsymbol{b}_a \times \boldsymbol{b}_b \rangle \cdot \hat{\boldsymbol{x}}_s. \tag{23}$$

Now we can justify our earlier claim that the first term in Eq. (19) dominates: using the estimates in Eq. (22), the first term is of order $D_{\rm TeV}^2 D_e^2 B^2/D_s^2$, whereas the second term is of order $D_{\rm e}^4 B^2/D_s^2$ which is smaller by the factor $D_e^2/D_{\rm TeV}^2 \sim 10^{-6}$. Therefore

$$Q_\infty \approx \sum \frac{q_a q_b D_{\rm TeV,a} D_{\rm TeV,b}}{E_{ea} E_{eb} D_s^2} \langle \boldsymbol{b}_a \times \boldsymbol{b}_b \rangle \cdot \hat{\boldsymbol{x}}_s, \tag{24}$$

where we use the notation $E_{ea} = E_e(E_a)$.

Eq. (1) gives

$$\langle \boldsymbol{b}_a \times \boldsymbol{b}_b \rangle \cdot \hat{\boldsymbol{x}}_s = \int_{t_{ia}}^{t_{ICa}} dt' \int_{t_{ib}}^{t_{ICb}} dt''\ \hat{\boldsymbol{x}}_s \cdot (\boldsymbol{x}_a(t') - \boldsymbol{x}_b(t'')) M_H(|\boldsymbol{x}_a(t') - \boldsymbol{x}_b(t'')|), \tag{25}$$

where

$$\boldsymbol{x}_a(t') = \boldsymbol{x}_a(t_i) + \boldsymbol{v}_{ia}(t' - t_{ia}), \tag{26}$$

and similarly for $\boldsymbol{x}_b(t'')$. Under the approximation that all deflection angles are small, we get

$$\langle \boldsymbol{b}_a \times \boldsymbol{b}_b \rangle \cdot \hat{\boldsymbol{x}}_s \approx \int_{t_{ia}}^{t_{ICa}} dt' \int_{t_{ib}}^{t_{ICb}} dt'' d_{ab} M_H(|d_{ab}|), \tag{27}$$

where

$$d_{ab} \equiv (r_{ia} - (t'_a - t_{ia})) - (r_{ib} - (t''_b - t_{ib})). \tag{28}$$

We can simplify further by using $r_{ia} \gg t''_a - t_{ia}$ $(a = 1, 2, 3)$, which then implies $d_{ab} \approx r_{ia} - r_{ib}$ independent of the time integration variables. If $(d_{ab} - (r_{ia} - r_{ib}))M'_H(d_{ab}) \ll M_H(d_{ab})$ where the prime on M_H denotes differentiation with respect to the argument, then the integrand in Eq. (25) is approximately a constant and

$$\langle \boldsymbol{b}_a \times \boldsymbol{b}_b \rangle \cdot \hat{\boldsymbol{x}}_s \approx 2 D_{ea} D_{eb} (r_{ia} - r_{ib}) M_H(|r_{ia} - r_{ib}|), \tag{29}$$

where, $D_{ea} = D_e(E_a) = t_{ICa} - t_{ia}$, the time between pair production and IC scattering. To get a sense of numerical values, for the energies of interest, $D_{ea} \sim 30$kpc and $r_{i1} \sim r_{i2} \sim$ Gpc, and $r_{i1} - r_{i2} \sim$ Mpc.

Finally we have the simple result

$$Q_\infty \approx \frac{2e^2}{D_s^2} \sum_{(a,b)} \frac{q_{ab} D_{\rm TeV,a} D_{\rm TeV,b} D_{ea} D_{eb}}{E_{ea} E_{eb}} d_{ab} M_H(|d_{ab}|), \tag{30}$$

where $q_{ab} = +1$ if $q_a = q_b$ and $q_{ab} = -1$ if $q_a \neq q_b$.

Note that

$$d_{ab} \approx r_{ia} - r_{ib} = (r_s - D_{\rm TeV,a}) - (r_s - D_{\rm TeV,b}) = D_{\rm TeV,b} - D_{\rm TeV,a} < 0, \tag{31}$$

for $E_a < E_b$.

We now express Q_∞ in terms of the observed energies. First we use Eq. (4) that gives us the time between pair production and IC scattering,

$$D_e(E) \approx \frac{178\ {\rm kpc}}{(1+z_s)^4} \left(\frac{10\ {\rm GeV}}{E}\right)^{1/2} \equiv \left(\frac{\delta_e}{E}\right)^{1/2}, \tag{32}$$

where $\delta_e \approx 3.2 \times 10^5/(1+z_s)^8$ GeV-kpc^2 $\approx 4.8 \times 10^{34}/(1+z_s)^8$ Gpc since we are working in natural units and we used $z_e \approx z_s$.

Similarly

$$D_{\rm TeV} = \frac{237\ {\rm Mpc}}{(1+z_s)^2} \left(\frac{10\ {\rm GeV}}{E}\right)^{1/2} \equiv \left(\frac{\delta_T}{E}\right)^{1/2}, \tag{33}$$

where $\delta_T \approx 5.6 \times 10^5/(1+z_s)^4$ GeV-Mpc^2 $\approx 8.8 \times 10^{40}/(1+z_s)^4$ Gpc. We can assume $z_s \approx z_e$. Also,

$$E_e(E) \approx 1.7\ {\rm TeV} \left(\frac{E}{10\ {\rm GeV}}\right)^{1/2} \equiv \left(\frac{E}{\epsilon_e}\right)^{1/2}, \tag{34}$$

with $\epsilon_e \approx 3.5 \times 10^{-6}$ GeV^{-1}.

Then,

$$\begin{aligned} Q_\infty &= -\frac{2e^2 \delta_e \delta_T \epsilon_e}{D_s^2} \left[\frac{q_{12}|d_{12}| M_H(|d_{12}|)}{E_1^{3/2} E_2^{3/2}} + \frac{q_{23}|d_{23}| M_H(|d_{23}|)}{E_2^{3/2} E_3^{3/2}} - \frac{q_{13}|d_{13}| M_H(|d_{13}|)}{E_3^{3/2} E_1^{3/2}} \right] \\ &= -\frac{10^{27}}{(1+z_s)^{12} {\rm G}^2} \left[\frac{q_{12}|d_{12}| M_H(|d_{12}|)}{\mathcal{E}_1^{3/2} \mathcal{E}_2^{3/2}} + \frac{q_{23}|d_{23}| M_H(|d_{23}|)}{\mathcal{E}_2^{3/2} \mathcal{E}_3^{3/2}} - \frac{q_{13}|d_{13}| M_H(|d_{13}|)}{\mathcal{E}_3^{3/2} \mathcal{E}_1^{3/2}} \right] \left(\frac{1\ {\rm Gpc}}{D_s}\right)^2, \end{aligned} \tag{35}$$

where we have used $e^2 = 4\pi/137$, the Gauss to GeV conversion 1 G $= 1.95 \times 10^{-20}$ GeV^2, and denoted $\mathcal{E}_a = E_a/10$ GeV.

Finally we can write the distances d_{ab} in terms of the energies, since d_{ab} is the distance between the points where pair production occurs for photons of observed energy E_a and E_b. Using Eq. (3) together with Eq. (5),

$$d_{ab} \approx r_{ia} - r_{ib} = -\frac{237\kappa}{(1+z_s)^2}\left(\frac{1}{\sqrt{\mathcal{E}_a}} - \frac{1}{\sqrt{\mathcal{E}_b}}\right) \text{ Mpc}. \tag{36}$$

Eqs. (35) and (36) specify the correlator Q_∞, *i.e.* the value of $Q(R)$ in Eq. (8) for large values of R in the case when only cascade photons are present. The only required inputs are the helical magnetic correlation function and the gamma ray energies that are observed. Let us now consider $Q(R)$ for smaller values of R, still only considering cascade photons. It is useful to rewrite Eq. (8) as

$$Q(R) = \langle (\boldsymbol{n}(E_1) - \boldsymbol{n}(E_3)) \times (\boldsymbol{n}(E_2) - \boldsymbol{n}(E_3)) \cdot \boldsymbol{n}(E_3) \rangle_R. \tag{37}$$

Then it is clear that $Q(R)$ depends on the length of the vector $\boldsymbol{n}(E_1) - \boldsymbol{n}(E_3)$ and $\boldsymbol{n}(E_2) - \boldsymbol{n}(E_3)$ where $\boldsymbol{n}(E_1)$ and $\boldsymbol{n}(E_2)$ are restricted to lie in the patch of size R with $\boldsymbol{n}(E_3)$ as center. The average lengths of these vectors are proportional to R for small R. Further, the cascade photons are clustered in the region around $\boldsymbol{n}_3$ and so the lengths do not grow indefinitely as R increases. For R larger than the typical bending angles of the cascade photons, the lengths can be taken to saturate. A functional form of $Q_c(R)$ that takes the lengths of the vectors $\boldsymbol{n}(E_1) - \boldsymbol{n}(E_3)$ and $\boldsymbol{n}(E_2) - \boldsymbol{n}(E_3)$ into account in a patch of radius R is

$$Q_c(R) = (1 - e^{-R/\Theta(E_1)})(1 - e^{-R/\Theta(E_2)})Q_\infty. \tag{38}$$

2.2 Charge ambiguity

The formula for Q_∞, Eq. (35), includes the factors $q_{ab} = \pm 1$, that depend on whether the cascade photons at energies E_a and E_b originated from like charges (electron-electron or positron-positron) or unlike charges. The ambiguity can be traced back to the Lorentz force formula that is invariant under charge reversal together with magnetic field reversal. We now discuss how to possibly resolve the ambiguity due to the q_{ab} factors in connecting observed $Q_c(R)$ to the helical power spectrum M_H.

Let us assume that data are sufficiently precise that we can measure $Q_c(R, E_a, E_b, E_c)$ for a wide range of energies. Then consider $Q_c(R, E_a, E_b, E_c)$ and $Q_c(R, E'_a, E_b, E_c)$ where $E'_a \neq E_a$. By continuity, we expect $Q_c(R, E_a, E_b, E_c) \approx Q_c(R, E'_a, E_b, E_c)$, and if this is indeed observed to be the case, then $q_a = q'_a$. If, however, $Q_c(R, E_a, E_b, E_c)$ and $Q_c(R, E'_a, E_b, E_c)$ are sharply different, then $q_a = -q'_a$. In other words, to connect observed Q_c to M_H we need to consider the different discrete possibilities and then choose the signs so as to reconstruct a continuous M_H[3].

The above resolution assumes very extensive observational data. Even without such data but with the prior that the magnetic field is smooth on the scales of interest, we can take $q_{ab} = +1$ since without field reversals the cascades at different energies must arise from like charges. In what follows, we will assume $q_{ab} = +1$.

2.3 Source plus background

The diffuse gamma ray sky contains cascade photons from many different TeV blazars, as well as non-cascade photons from other sources. The expression for $Q_c(R)$ in Eq. (38) was derived for cascade gamma rays from a single TeV blazar, assuming no contamination from other TeV blazars or non-cascade photons. We now extend our calculation to include non-cascade photons.

The ensemble average over photons in some given patch of radius R will include both cascade, *i.e.* signal, and non-cascade, *i.e.* noise, photons. The value of $Q(R)$ will depend on the ratio of cascade to non-cascade photons within that patch. The number of non-cascade photons within the patch will be proportional to the area of the patch

$$N_n(E, R) = 2\pi\sigma_n(E)(1 - \cos R) \equiv \sigma_n(E)A(R), \tag{39}$$

where $\sigma_n(E)$ is the average areal density of such "noise" photons with energy E, and the area of a patch of radius R on a unit sphere is $A(R) = 2\pi(1 - \cos R)$.

The number of cascade photons within a patch of radius R is also proportional to the area of the patch when R is less than the typical spread of cascade photons. For larger R, the number of cascade photons within the patch stays constant. This suggests

$$N_c(E) = N_\infty(E)(1 - e^{-A(R)/A(\Theta(E))}), \tag{40}$$

where $N_\infty(E)$ is the number of cascade photons of energy E when the patch size is large, and $\Theta(E)$ is the typical bending angle at energy E. We stress that these functional forms have the correct asymptotic dependencies but their precise shape should not be taken too literally.

[3] The discrete ambiguity is similar to the one that occurs when reconstructing magnetic fields using Faraday Rotation measurements (Zeldovich et al. 1983).

Then $Q(R)$, which is an average over all photons – cascade and non-cascade – will be given by

$$Q(R) = \frac{N_c(E_1)N_c(E_2)N_c(E_3)}{N_t(E_1)N_t(E_2)N_t(E_3)} Q_c(R), \tag{41}$$

where $N_t = N_c + N_n$.

Note that in a given patch we only consider a single E_3 photon that is located at the center of the patch, but then $Q(R)$ is also averaged over all patches, some of which may be centered on E_3 photons that are not from a cascade. This gives the energy E_3 a special status, and N_c/N_t for E_3 is the average number of cascade to non-cascade photons of energy E_3 over the region of sky under consideration *e.g.* after the Milky Way has been masked out. So N_c/N_t for E_3 is just a numerical factor; in particular, it does not depend on the radius of the patch. In reconstructing the helical power spectrum from $Q(R)$, the value of $N_c(E_3)/N_t(E_3)$ will be a scaling factor. In what follows, we will denote

$$\frac{N_c(E_3)}{N_t(E_3)} = \frac{1}{1+\nu_3} \tag{42}$$

where ν_3 is independent of R.

The ratio $N_c(E)/N_t(E)$ $(E = E_1, E_2)$ depends on the radius of the patch and on the dimensionless ratio,

$$\nu(E) \equiv \frac{\sigma_n(E) A(\Theta(E))}{N_\infty(E)(1-e^{-1})}, \tag{43}$$

which is the ratio of the number of noise to the number of signal photons in a patch of angular radius $\Theta(E)$, *i.e.* the "noise to signal ratio at energy E". Then,

$$\frac{N_c}{N_t} = \left(1 + \frac{0.63\ \nu(E)\mathcal{A}(R,E)}{1-\exp(-\mathcal{A}(R,E))}\right)^{-1}, \tag{44}$$

where $\mathcal{A}(R,E) = A(R)/A(\Theta(E)) = (1-\cos R)/(1-\cos\Theta(E))$. Since the shape of $Q(R)$ is sensitive to $\nu(E)$, observations of $Q(R)$ may in principle be used to determine $\nu(E)$ which would give a handle on the relative number of cascade and non-cascade photons and also the number of TeV blazar sources. In the simplified analysis we present here, we will assume $\nu(E) \sim 1$ and independent of the energy E.

In Fig. 3 we plot $Q(R)/Q_\infty$ for sample parameters, showing that we expect magnetic helicity to lead to a peak in $Q(R)$. The location of the peak does not depend on the magnetic helicity power spectrum, M_H, but does depend on the normal power spectrum, M_N, via the bending angles, $\Theta(E)$. The shape of the plots in Fig. 3 can be understood as follows. Since $E_1 < E_2$, and $\Theta(E) \propto E^{-3/2}$ from Eq. (6), we have $\Theta(E_2) < \Theta(E_1)$. For $R \ll \Theta(E_2)$ the factors N_c/N_t are approximately independent of R and the exponential factors in Eq. (38) can be expanded to get $Q(R) \sim R^2$. For $R \sim \Theta(E_2)$, N_c/N_t at E_1 is still independent of R since $R/\Theta(E_1)$ is small, but the N_c/N_t factor for E_2 starts to vary with R if

$$\frac{0.63\ \nu(E_2)\mathcal{A}(R,E_2)}{1-\exp(-\mathcal{A}(R,E_2))} > 1, \text{ and, } \mathcal{A}(R,E_2) > 1. \tag{45}$$

With $\nu(E) \approx 1$, these conditions are satisfied for $\mathcal{A}(R,E_2) \approx 1$. Therefore N_c/N_t for E_2 decreases as $\sim 1/R^2$ for $R > R_*$ where $\mathcal{A}(R_*,E_2) \approx 1$ which gives

$$R_* \approx \Theta(E_2). \tag{46}$$

Thus the shape of $Q(R)$ is flat for $R \sim R_*$. For $\Theta(E_2) < R < \Theta(E_1)$, similarly we find $Q(R) \sim 1/R$, and finally for $\Theta(E_1) < R$, we get $Q(R) \sim 1/R^4$.

The important features of the shape of $Q(R)$ are that it has a peak located at

$$R_{\rm peak} \approx R_* \approx \Theta(E_2) \tag{47}$$

and the peak height is found by substituting $R = R_{\rm peak}$ in Eq. (41) and using Eqs. (38) and (35),

$$Q_{\rm peak} \approx \frac{0.63}{(1+0.63\nu_1)(1+\nu_2)(1+\nu_3)} \frac{\Theta(E_2)}{\Theta(E_1)} Q_\infty \approx 0.1 \left(\frac{E_1}{E_2}\right)^{3/2} Q_\infty \tag{48}$$

where $\nu_i = \nu(E_i)$, with $\nu_i = 1$ in the final estimate, and we have assumed $\Theta(E_2) \ll \Theta(E_1)$. The amplitude of the peak depends on Q_∞, which depends on the magnetic helicity spectrum, M_H. In Sec. 3 we will consider some models of the helicity power spectra and plot $Q(R)$. In Sec, 4 we will use these peak characteristics to estimate the intergalactic magnetic field strength.

3 SAMPLE MODELS OF M_H

We now calculate $Q(R)$ from Eq. (41) with Q_c given by Eq. (38) and Q_∞ by Eq. (35) with $q_{ab} = 1$ (see Sec. 2.2). For simplicity, we assume a power-law form for the helical power spectrum,

$$rM_H(r) = B_N^2 \frac{r}{r_N} \left(\frac{|r|}{r_N}\right)^n, \tag{49}$$

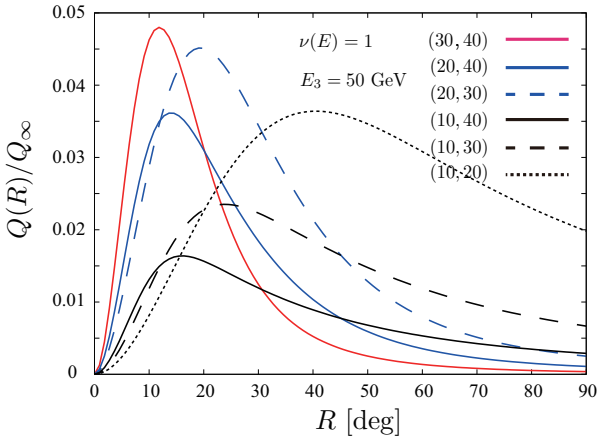

Figure 3. Plot of $Q(R)/Q_\infty$ for $E_3 = 50$ GeV and (E_1, E_2) as shown for $\nu(E) = 1$, and with $B = 2 \times 10^{-13}$ G and $D_s = 1$ Gpc to estimate $\Theta(E)$. The lines in black, blue and red are for $E_1 = 10$, 20 and 30 GeV, respectively. The dotted, dashed and solid lines are for $E_2 = 20$, 30 and 40 GeV. Note that the peaks in the curves with the same E_2 are at approximately the same location.

where B_N is the normalized magnetic field strength at the normalization scale r_N. In our context, B_N is defined at a redshift z_s since that is roughly where the cascade is being produced. The conversion to the comoving magnetic field strength B_0 is $B_0 = B_N/(1+z_s)^2$. We adopt $B_N = 2\times10^{-13}$ G and $r_N = 100$ Mpc. According to Eq. (1), $n = -1$ represents a scale-invariant helicity spectrum, $n > -1$ gives a red-tilted spectrum, and $n < -1$ gives a blue-tilted spectrum. The choice of B_N is made to match the peak scale of the energy combination (10,40) as seen in the Fermi-LAT data ($R_* \approx 14^\circ$) in Tashiro et al. (2014). The plots of $Q(R)$ versus R are shown in Fig. 4.

Whereas we have adopted the form in Eq. (49) and predicted $Q(R)$, we can also reverse these arguments and deduce $M_H(r)$ from observational data.

4 CONCLUSIONS

In this paper we have related the statistics, $Q(R)$, calculated from the diffuse gamma ray sky, to the helical power spectrum, M_H, of intergalactic magnetic fields. Our results show that helical intergalactic magnetic fields lead to a peak structure in $Q(R)$. The angular location of the peak determines the typical bending angle of cascade photons of a given energy, and is in turn related to the non-helical power spectrum, M_N, of the magnetic field; the amplitude of the peak is related to the helical power spectrum, M_H. The sign of Q depends on the handedness of the magnetic field and, except when there is a lot of power on small distance scales, we expect $Q < 0$ for left-handed fields. In addition, the shape of $Q(R)$ is sensitive to the fraction of cascade to non-cascade photons in the sky, thus possibly providing a tool to study the distribution and properties of cascade photons from TeV blazars.

Using our results, we can obtain a numerical estimate of the helical power spectrum. From Eq. (35) we estimate

$$|\, d_{12} M_H(|d_{12}|)\,| \sim (3\times10^{-16}\ \mathrm{G})^2 \mathcal{E}_1^{3/2}\mathcal{E}_2^{3/2} \left(\frac{D_s}{1\ \mathrm{Gpc}}\right)^2 \left(\frac{Q_\infty}{10^{-4}}\right)(1+z_s)^{12} \sim \left[1.5\times10^{-14} D_{s1}(1+z_s)^6\ \mathrm{G}\right]^2, \qquad (50)$$

where, in the last estimate we have used $E_1 = 10$ GeV, $E_2 = 40$ GeV, *i.e.* $\mathcal{E}_1 = 1$, $\mathcal{E}_2 = 4$, $Q_{\rm peak} = 3\times10^{-4}$ (Tashiro et al. 2014), $Q_\infty = 80\ Q_{\rm peak}$ from Eq. (48) with $\nu(E_i) = 1$, and denoted $D_{s1} = D_s/1$ Gpc. Therefore we estimate

$$B_0 \approx 1.5\times10^{-14} D_{s1}(1+z_s)^4\ \mathrm{G}, \quad \text{from peak amplitude} \qquad (51)$$

where B_0 is the magnetic field strength at the present epoch and we have taken the field strength to evolve in proportion to $(1+z)^2$. From Tashiro et al. (2014) we find that the peak in $Q(R)$ is located at $\Theta_s \approx 14^\circ$ when $E_1 = 10$ GeV, $E_2 = 40$ GeV. Then from Eq. (6), with $E_\gamma = 40$ GeV – recall that the peak position is determined by E_2 as in Eq. (47) – we find

$$B_0 \approx 8\times10^{-14} D_{s1}(1+z_s)^4\ \mathrm{G}, \quad \text{from peak location} \qquad (52)$$

This rough agreement between the two independent estimates in Eq. (51) and Eq. (52) is quite remarkable and suggests that the intergalactic magnetic fields are significantly, if not maximally, helical.

In conclusion, we have developed the connection between our proposed parity odd correlator, $Q(R)$, and properties of the intergalactic magnetic field. We find encouraging agreement between independent estimates of the magnetic field strength using observed data, thus providing further confidence in the robustness of the signal discussed in Tashiro et al. (2014). There is also some tentative indication in the observed $Q(R)$ to peak at smaller angles at higher E_2 (Tashiro et al. 2014) which is in

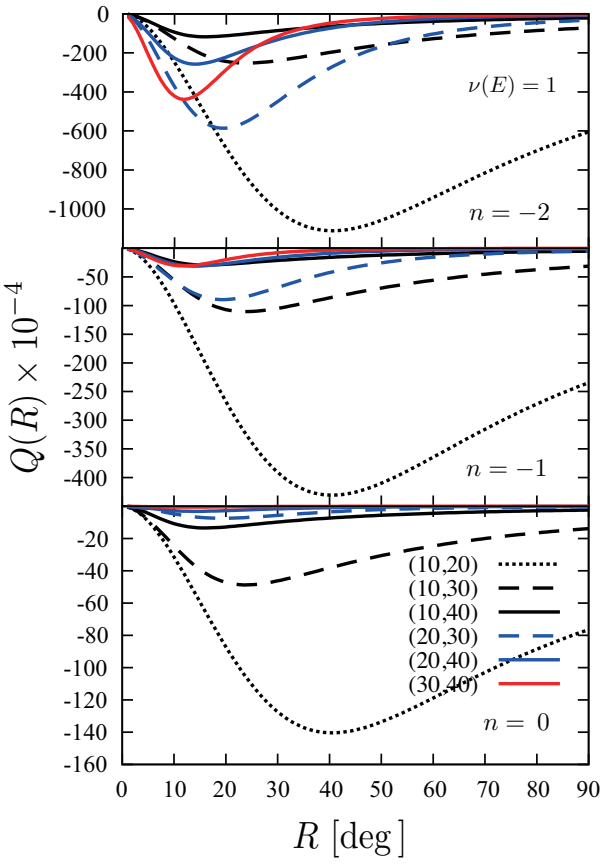

Figure 4. Plot of $Q(R)$ for different spectral index n of M_H. We set $\nu(E) = 1$. From the top to bottom panels, the spectral index is set to $n = -2$, -1 and 0, respectively. The energy combinations are represented with the same types of lines as in Fig. 3.

agreement with the trend in Fig. 4. Another interesting observation is that if we combine Eq. (48) and Eq. (35) and assume that the first term in Eq. (35) dominates, we find

$$Q_{\rm peak} \sim -\frac{10^{26}}{(1+z_s)^{12}{\rm G}^2}\frac{q_{12}|d_{12}|M_H(|d_{12}|)}{\mathcal{E}_2^{3/2}}\left(\frac{1\ {\rm Gpc}}{D_s}\right)^2 . \tag{53}$$

Hence, for a scale invariant spectrum, $Q_{\rm peak}$ depends only on E_2 and there is little dependence on E_1. We have also seen that $R_{\rm peak}$ is independent of E_1 (see Eq. (47)). Thus both $R_{\rm peak}$ and $Q_{\rm peak}$ are only sensitive to E_2 for a spectrum that is not too steep. Indeed, in the plots obtained from Fermi data for $E_2 = 40$ GeV there is a peak with amplitude $\sim 3 \times 10^{-4}$ at roughly $R = 14^\circ$ regardless of the value of E_1, again showing consistency with the intergalactic magnetic fields hypothesis. Further, Eq. (47) predicts that $Q(R)$ will peak at $R \approx 21^\circ$ when $E_2 = 30$ GeV and at $R \approx 40^\circ$ when $E_2 = 20$ GeV; the height of the peak is sensitive to the noise to signal ratio, $\nu(E)$, and to the helicity power spectrum.

We close with a few cautionary remarks. Our analytic methods have been possible only because we have made several simplifying assumptions along the way. For example, we have ignored the stochasticity of the pair production – which depends on the EBL spectrum – and the CMB up-scattering processes. Monte Carlo methods seem to be most suitable for including these processes though simulations will be challenging because of the range of length scales involved (kpc to Gpc). We hope the rewards of discovering helical intergalactic magnetic fields and the enormous implications for particle physics and cosmology will spur further investigations.

ACKNOWLEDGEMENTS

We are grateful to Wenlei Chen, Francesc Ferrer, and Andrew Long for comments. TV thanks IAS, Princeton for hospitality while this work was being done. This work was supported by MEXT's Program for Leading Graduate Schools "PhD professional: Gateway to Success in Frontier Asia," the Japan Society for Promotion of Science (JSPS) Grant-in-Aid for Scientiffic Research (No. 25287057) and the DOE at ASU.

APPENDIX A: SIGN OF Q, M_H AND MAGNETIC HANDEDNESS

Define

$$C_{ij} = \frac{1}{2}\langle B_i(\boldsymbol{x}+\boldsymbol{r})B_j(\boldsymbol{x}) - B_j(\boldsymbol{x}+\boldsymbol{r})B_i(\boldsymbol{x})\rangle = \epsilon_{ijl}r^l M_H(r). \tag{A1}$$

Then

$$r_k\epsilon^{kij}C_{ij} = 2r^2 M_H(r). \tag{A2}$$

Let us evaluate the left-hand side directly for a right-handed magnetic field configuration. Take $\boldsymbol{x}=0$, $\boldsymbol{r}=r\hat{\boldsymbol{z}}$ ($r>0$), $\boldsymbol{B}(\boldsymbol{x}=0)=B\hat{\boldsymbol{x}}$, and $\boldsymbol{B}(\boldsymbol{x}=r\hat{\boldsymbol{z}})=B\hat{\boldsymbol{y}}$. This is a right-handed configuration because the magnetic field rotates counterclockwise as one goes from the origin to $r\hat{\boldsymbol{z}}$. Then

$$2r^2M_H(r) = r_k\epsilon^{kij}C_{ij} = r\hat{\boldsymbol{z}}\cdot\boldsymbol{B}(r\hat{\boldsymbol{z}})\times\boldsymbol{B}(0) = rB^2\hat{\boldsymbol{z}}\cdot\hat{\boldsymbol{y}}\times\hat{\boldsymbol{x}} = -rB^2 < 0. \tag{A3}$$

So we find, with our conventions, $M_H(r)<0$ for a right-handed magnetic field configuration.

From Eq. (35), assuming that the lowest energy photon term dominates,

$$Q \sim -\frac{2e^2\delta_e\delta_T\epsilon_e}{D_s^2}\frac{q_{ab}|d_{ab}|M_H(|d_{ab}|)}{E_a^{3/2}E_b^{3/2}}. \tag{A4}$$

Therefore, if $q_{ab}=+1$ as for smooth fields, $Q<0$ implies $M_H>0$ which implies left-handed magnetic helicity with our conventions. This conclusion is reversed if $q_{ab}=-1$ or if the helical spectrum is such that the last term in Eq. (35) dominates, which could happen if there is significant power on small scales.

REFERENCES

Aharonian F., et al. (Fermi-LAT Collaboration), 2006, Nature, 440, 1018.
Aharonian F. A., Coppi P. S., Voelk H. J., 1994, Astrophys. J. Lett., 423, L5.
Broderick A. E., Chang P., Pfrommer C., 2012, Astrophys. J., 752, 22.
Chu Y.-Z., Dent J. B., Vachaspati T., 2011, Phys. Rev. D, 83, 123530.
Copi C. J., Ferrer F., Vachaspati T., Achúcarro A., 2008, Phys. Rev. Lett., 101, 171302.
Dolag K., Kachelrieß M., Ostapchenko S., Tomàs R., 2009, Astrophys. J., 703, 1078.
Dolag K., Kachelriess M., Ostapchenko S., Tomàs R., 2011, Astrophys. J. Lett., 727, L4.
Elyiv A., Neronov A., Semikoz D. V., 2009, Phys. Rev. D, 80, 023010.
Gould R. J., Schréder G., 1966, Phys. Rev. Lett., 16, 252.
Kahniashvili T., Vachaspati T., 2006, Phys. Rev. D, 73, 063507.
Long A. J., Sabancilar E., Vachaspati T., 2014, JCAP, 2, 36.
Miniati F., Elyiv A., 2013, Astrophys. J., 770, 54.
Monin A. S., I'Aglom A. M., 1971, Statistical fluid mechanics; mechanics of turbulence.
Neronov A., Semikoz D. V., 2007, J. Exp. Theor. PHys. Lett., 85, 473.
Neronov A., Semikoz D. V., 2009, Phys. Rev. D, 80, 123012.
Neronov A., Vovk I., 2010, Science, 328, 73.
Plaga R., 1995, Nature, 374, 430.
Rees M. J., 1987, Royal Astronomical Society, Quarterly Journal, 28, 197.
Schlickeiser R., Ibscher D., Supsar M., 2012, Astrophys. J., 758, 102.
Tashiro H., Chen W., Ferrer F., Vachaspati T., 2014, Month. Not. R. Astro. Soc., 445, L41.
Tashiro H., Vachaspati T., 2013, Phys. Rev. D, 87, 123527.
Tavecchio F., Ghisellini G., Foschini L., Bonnoli G., Ghirlanda G., Coppi P., 2010, Month. Not. R. Astro. Soc., 406, L70.
Vachaspati T., 2001, Phys. Rev. Lett., 87, 251302.
Zeldovich I. B., Ruzmaikin A. A., Sokolov D. D., 1983, Magnetic fields in astrophysics.